Enhancing Cu_2ZnSnS_4 Solar Cell Efficiency through Antimony Substitution for Tin: A SCAPS-1D Simulation Study

Sushmita Chaudhari, and Kannan P. K.

***Abstract*— SCAPS-1D, a one-dimensional solar cell simulator, provides a valuable tool for predicting device performance based on layer-by-layer material properties. Copper Zinc Tin Sulfide (CZTS) has emerged as a promising absorber material due to its exceptional light absorption coefficient and the abundance and non-toxic nature of its constituent elements. This study leverages SCAPS-1D to investigate the working mechanism of CZTS-based solar cells. We simulate a Mo/CZTS/CdS/ZnO device structure under AM 1.5 spectrum illumination and 300 K temperature, analyzing the impact of individual layer thickness on photovoltaic performance. Further, a comparative analysis explores the influence of various n-type materials. In addition, the introduction of antimony (Sb) doping into CZTS leads to a significant change in efficiency of the cell. The efficiency of Sb-doping CZTS attained 21.90%, while there was a great improvement by 3% via reduced recombination losses and enhanced photocurrent. This work gives an insight into the possibility of Sb doping for the improvement in the performance of thin-film solar cells.**

Link to graphical and video abstracts, and to code: https://latamt.ieeer9.org/index.php/transactions/article/view/9125

***Index Terms*— Photovoltaic cell, SCAPS-1D, CZTS, CdS, ZnO, Thin film.**

I. Introduction

THE increasing demand for clean and sustainable energy sources has driven significant research into renewable energy technologies. Among these, solar photovoltaics (PV) hold immense promise due to their ability to convert sunlight directly into electricity. Theoretically, only a small fraction of the Earth's surface covered with efficient solar cells could meet global energy demands. While solar PV accounted for roughly 8.3% of global electricity generation in 2024 [1], further efficiency improvements can significantly reduce production costs and make solar a viable alternative to fossil fuel-based power generation. Common thin film solar cell absorber materials are CdTe, ZnSe, Sb_2S_3, ZnTe and CZTS [2-9]. Among all Copper Zinc Tin Sulfide (CZTS, Cu_2ZnSnS_4) has emerged as a promising candidate for second-generation thin-film solar cells. Its high absorption coefficient, earth-abundant and non-toxic constituents, and direct bandgap make it an attractive substitute for currently used CdTe/CdSe-based thin-film solar cells. However, the maximum reported efficiencies for CZTS solar cells is around is around 10% and 12.6% for a CZTS and CZTSSe based solar cell solar cell [10-12] remain lower than those achieved with CIGS (Copper Indium Gallium Selenide) technology and theoretical predictions for CZTS.

Several deposition methods, both vacuum-based (sputtering [13], E-beam evaporation [14-15] etc.) and non-vacuum-based (dip coating [16-18], spin coating [19], electrodeposition [20-23], chemical bath deposition [24], combination technique of electrodeposition followed with chemical bath deposition [25] etc.), can be used to fabricate CZTS absorber layers. However, the performance of a solar cell depends not only on the absorber material but also on the other constituent layers, such as the buffer layer, window layer, and electrical contacts. These elements influence factors like band structure at heterojunctions and overall device functionality. In addition, there are several disadvantages of experimental methods such as cost inefficient, time inefficient etc. Optimizing parameters using experimental approach is very challenging and sometimes leading to inconsistent results. Secondly, reproducibility in various environmental or experimental conditions is also a biggest challenge. Hence in this study simulation is preferred as an invaluable tool instead of experimental approach before moving to experimental validity.

Researchers often use the SCAPS 1D simulation tool for optimize thin film solar cell performance. It facilitates the study of the effect of different parameters for example layer thickness, doping concentration etc. on the performance of device characteristics like QE, FF, Voc and Jsc. This make SCAPS 1D an important tool in solar cell design and optimization strategies. Specifically, researchers have been working to optimize second generation thin film solar cell using SCAPS 1D, including ZnTe based solar cell [7-8], CdTe based solar cell [2-3], ZnSe based solar cell [4] and CZTS based solar cell [9]. In case of CZTS various dopants have been reported with the view to minimizing the defects in Cu_2ZnSnS_4 (CZTS) and thereby improve the photocurrent of solar cells. Of these, antimony (Sb) has received much interest because of its ability to replace tin (Sn) within the CZTS crystal structure. This substitution also results in the formation, of an intermediate band about 0.5 eV below the valence band [26]. The existence of this intermediate band

The associate editor coordinating the review of this manuscript and approving it for publication was Diego Rivelino Espinoza-Trejo (*Corresponding author: Sushmita Chaudhari*).

Sushmita Chaudhari gratefully acknowledge MITS Gwalior for providing funding through the IRS scheme 2021 for this project and Marc Burgelman from Gents University in Belgium's department of electronics and information systems for generously providing the software free of cost.

Sushmita Chaudhari is with Department of Computer Science and Engineering, Brainware University Barasat, Kolkata-700125, West Bengal India (e-mail: sushmita.chaudhari@gmail.com).

Kannan P. K. is with Department of Physics, PSG Institute of Technology and Applied Research Coimbatore-641062, Tamil Nadu, India (e-mail: kannan@psgitech.ac.in).

improves light absorption and photocurrents, which will enhance the conversion ability of the solar cell. To best of our knowledge, no one has yet studied the impact of substitution of Sb for Sn in CZTS based solar cell on the device performance using SCAPS 1D.

Thus in the current study our main objective is to simulate Mo/CZTS/CdS/ZnO solar cell using SCAPS-1D and study its different parameters like efficiency (η), short circuit current (Jsc), open circuit voltage (V_{oc}) and fill factor (FF). The study is made using I-V Characteristics to predict the best possible efficiency by varying different parameters of cell like thickness of each layer (absorber layer, window layer and buffer layer) and the impact of different buffer layer materials. To enhance the efficiency of solar cell conversion, dopants are commonly employed in the absorber layer. Recently, Zhang et al. [26] conducted first-principle calculations and observed an enhancement in the absorber coefficient of CZTS. Additionally, their findings demonstrate that antimony (Sb) has a preference for occupying the tin (Sn) sites, thereby reducing and preventing non-radiative recombination. This study aims to improve the efficiency of solar cells made by using earth abundant materials.

II. Device Structure & Simulation

This study investigates the performance of a Mo/CZTS/CdS/ZnO solar cell structure using SCAPS-1D, a one-dimensional solar cell simulator. SCAPS-1D is a freely available software program widely used by researchers and students for simulating solar cell characteristics. Developed by Prof. Marc Burgelman at Ghent University's Department of Electronics and Information Systems in Belgium, it incorporates models for various physical phenomena within the device, including generation, recombination, defect states, and carrier transport.

The simulated device architecture is depicted in Fig. 1. Here, CZTS serves as the light absorber layer, sandwiched between a molybdenum (Mo) back contact and a cadmium sulfide (CdS) buffer layer. A zinc oxide (ZnO) window layer completes the device structure. Material properties such as thickness, bandgap, carrier concentrations (electron and hole), and electron affinity are crucial for defining each layer in the device model. These parameters were chosen based on literature values and are presented in Table I [27].

To achieve realism with experimental findings, defects are introduced into the absorber layers and is mentioned in Table II [27]. In addition, the applied simulation parameters throughout the experiments are Series resistance (Rs) of 1 Ωcm² and Shunt resistance (Rsh) of 10^6 Ωcm². Illumination conditions were set to mimic standard reporting conditions using AM 1.5 spectrum with Input power density of 1000 W/m², Temperature of 300 K (room temperature) as specified in Fig. 1. Additionally, specific surface recombination parameters were employed for the front and back electrodes of the simulated device. The metal work function, electron surface recombination velocity and hole surface recombination velocity of front electrode are 5.0 eV, 10^5 cm/s and 10^7 cm/s respectively. Whereas the metal work function, electron surface recombination velocity and hole surface recombination velocity of back electrode are flat band (assumed ohmic contact), 10^7 cm/s and 10^5 cm/s respectively and is mentioned in Table III.

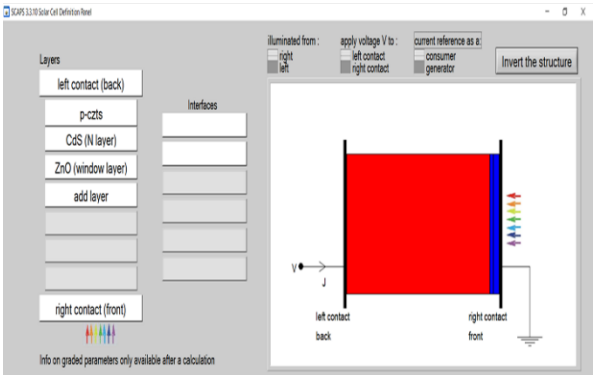

Fig. 1. Device structure of Mo/CZTS/CdS/ZnO solar cell.

TABLE I
MATERIALS PARAMETERS USED IN DESIGNING THE DEVICE STRUCTURE [27]

Parameters	*CZTS*	*CdS*	*ZnO*
Thickness	2	0.05	0.08
Bandgap (Eg)	1.5	2.4	3.3
Electron Affinity χ	4.5	4.5	4.6
Dielectric permittivity ε	10	10	9.0
CB density of state	2.2E18	2.2E18	2.2E18
VB density of state	1.8E19	1.8E19	1.8E19
Electron thermal velocity	1.0E7	1.0E7	1.0E7
Hole thermal velocity	1.0E7	1.0E7	1.0E7
Electron mobility	1.0E2	1.0E2	1.0E2
Hole mobility	2.5E1	2.5E1	2.5E1
Donor density	1.0E1	1.0E18	1.0E18
Acceptor density	1.0E18	0	1.0E1

III. Result and Discussion

To optimize the overall performance of CZTS based solar cell theoretical investigation on Mo/CZTS/CdS/ZnO cell is carried out using the software SCAPS-1D and the corresponding J-V curve of the cell is stored to calculate all the device parameters such as Voc, FF, Jsc, and η of the device.

Fig. 2 shows the J-V curve of Mo/CZTS/CdS/ZnO cell. From the figure it is clear that V_{oc}= 1.079229 volt and J_{sc}= 23.24 mA/cm² for the simulated cell, and thus

$$FF = \frac{V_{mp} * I_{mp}}{V_{oc} * I_{sc}} \approx 84.82\%$$

and its conversion efficiency η= Vmp*Imp/Pin ≈ 21.27%.

Fig. 3 depicts the simulated External Quantum Efficiency

(QE) of the Mo/CZTS/CdS/ZnO solar cell across the ultraviolet-visible (UV-Vis) spectrum. The high QE observed between 380 nm and 830 nm suggests efficient light absorption within this wavelength range, indicating the device's functionality primarily in the visible region. Quantum efficiency is reduced below 300 nm wavelength. It may be because in case of photons having energy higher than the bandgap of absorber material, excess energy will not be utilized for the charge carrier generation and will dissipate as thermal energy. This excess energy loss will reduce the overall photo conversion efficiency.

However, for optimal performance, considerations beyond light absorption are crucial. Fig. 4 illustrates the simulated band alignment at the critical CZTS/CdS interface, which forms a heterojunction between the absorber and buffer layer. As highlighted by Susanne et al. [28], a cliff-like band alignment, where the conduction band minimum (CBM) of CdS lies below that of CZTS, can lead to increased interface recombination due to a narrower bandgap at the junction compared to the bulk CZTS bandgap. This phenomenon, along with the spike-like band alignment at the CdS/ZnO interface, might be contributing factors to the relatively low conversion efficiency of 21.27% observed in Fig. 2 (compared to the theoretical potential of CZTS solar cells). The spike at the CdS/ZnO heterojunction, while potentially reducing interface recombination, can also act as a barrier for charge carrier transport, hindering efficient collection at the electrodes and ultimately limiting device performance.

A. Impact of Absorber Layer Thickness

Fig. 5 explores the relationship between absorber layer thickness (varied from 500 nm to 3000 nm in 500 nm steps) and key device parameters like efficiency (η), open-circuit voltage (Voc), fill factor (FF), and short-circuit current density (Jsc). The initial increase in efficiency with increasing thickness can be attributed to an enhanced light absorption probability, as confirmed by the rising ratio of absorbed photons to incident light. However, this trend is known to eventually reverse in practical devices, as reported in [29]. As the absorber layer thickness grows beyond a certain point, several factors can lead to a decrease in efficiency. One is Increased Recombination: With a thicker absorber layer, the generated charge carriers have to travel a longer distance to reach the collecting electrodes. This increases the probability of encountering recombination centers, such as defects or grain boundaries within the material, ultimately reducing the number of collected carriers and lowering efficiency. Second is Carrier Diffusion Length: The diffusion length represents the average distance a charge carrier can travel before recombining. If the absorber thickness exceeds the diffusion length, a significant portion of generated carriers may not reach the electrodes, again leading to efficiency losses. Therefore, an optimal absorber thickness exists that balances efficient light absorption with minimal carrier recombination.

B. Impact of Buffer Layer Thickness

Fig. 6 investigates the effect of buffer layer thickness (varied from 30 nm to 100 nm in 10 nm steps) on key device parameters like efficiency (η), short-circuit current density (J_{sc}), open-circuit voltage (Voc), and fill factor (FF). The observed increase in efficiency, Jsc and Voc with increasing buffer layer thickness can be attributed to its role in reducing recombination losses within the device. As buffer

TABLE II
DEFECTS PARAMETERS USED TO DESIGN CZTS MATERIAL PROPERTIES [27]

Defects	*Defect density Nt (cm^{-3})*	*Charge state: Type*	*Electron hole capture cross section ($\sigma e,\sigma h$) (cm^2)*	*Level*
Multivalent defect V_{Cu}, Cu_{Zn}	5E14	(0/-) acceptor	10^{-13},10^{-13}	0.1 eV above VBM VB tail
Multivalent defect Zn_{Sn}, Cu_{Sn}	5E14	(-2/-) acceptor	10^{-14},10^{-14}	0.2 eV above VBM VB tail
Multivalent defect V_{Sn}, Zn_{Sn}, Cu_{Sn}	5E14	(-2/-3) acceptor	10^{-14},10^{-14}	0.5 eV above VBM VB tail

TABLE III
SIMULATION PARAMETERS USED TO DESIGN CZTS MATERIAL PROPERTIES

Simulation Parameters	
Series resistance (Rs)	1 Ωcm²
Shunt resistance (Rsh)	10^6 Ωcm²
Illumination conditions	
Input power density	1000 W/m²
Temperature	300 K (room temperature)
Surface recombination parameters for Front electrode	
Metal work function:	5.0 eV
Electron surface recombination velocity	10^5 cm/s
Hole surface recombination velocity	10^7 cm/s
Surface recombination parameters for Back electrode	
Metal work function	Flat band (assumed ohmic contact)
Electron surface recombination velocity	10^7 cm/s
Hole surface recombination velocity	10^5 cm/s

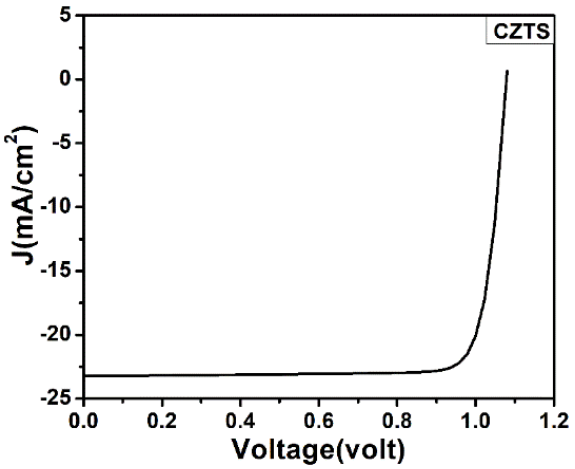

Fig. 2. J-V curve of Mo/CZTS/CdS/ZnO cell.

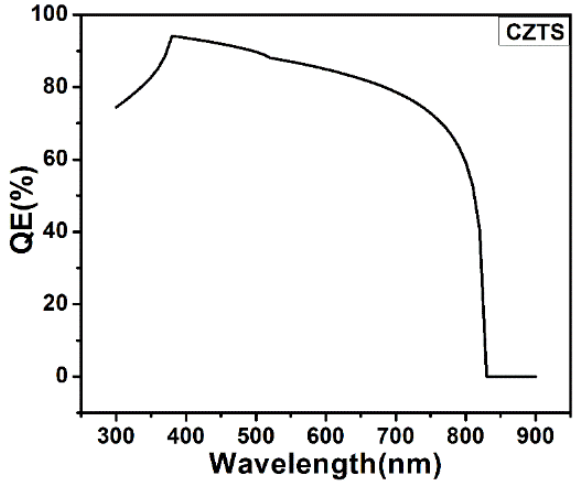

Fig. 3. Quantum Efficiency (QE) versus wavelength of Mo/CZTS/CdS/ZnO solar cell.

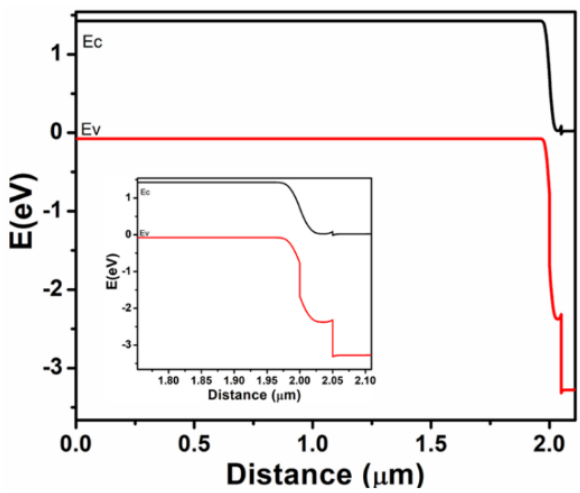

Fig. 4. Band alignment of Mo/CZTS/CdS/ZnO solar cell.

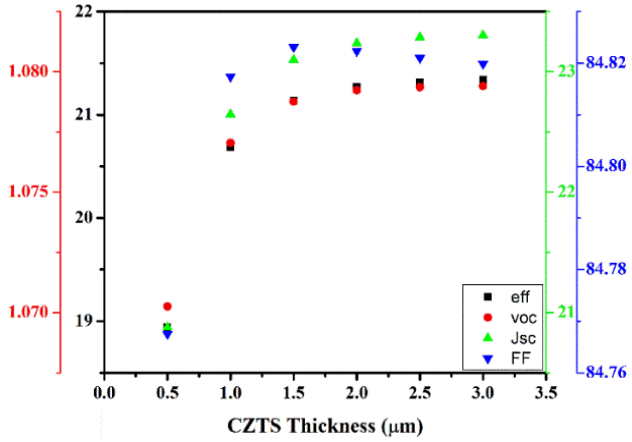

Fig. 5. Variation in device characteristics of Mo/CZTS/CdS/ZnO solar cell by varying thickness of CZTS layer.

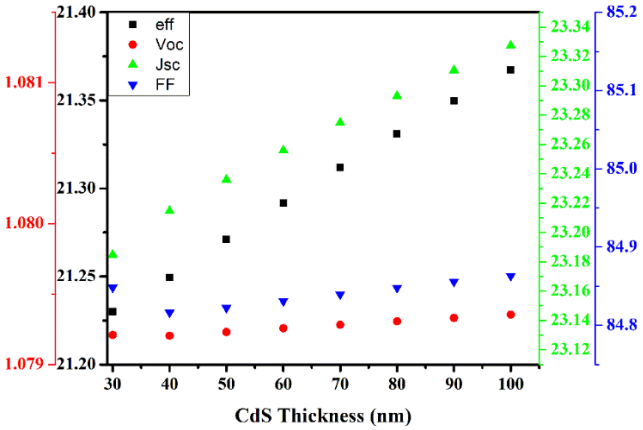

Fig. 6. Variation in device characteristics of Mo/CZTS/CdS/ZnO solar cell by varying thickness of CdS layer.

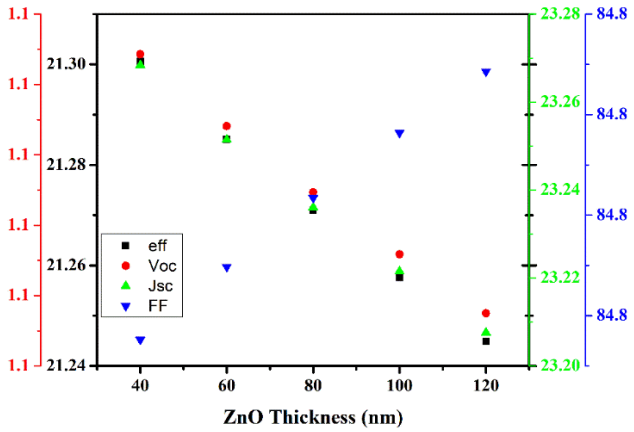

Fig. 7. Variation in device characteristics of Mo/CZTS/CdS/ZnO solar cell by varying thickness of ZnO layer.

layer's thickness increases, more photons are absorbed beyond the region of the hole diffusion length. This leads to a reduction in the recombination rate. This recombination would otherwise reduce the number of carriers available for current collection. However, it's important to note that excessively thick buffer layers can also have detrimental effects [30].

Fig. 7 highlights the influence of window layer thickness on device performance. From Fig. 7, it is clear that efficiency of cell not only pivot on the absorber layer's thickness or buffer layer but also depend upon the window layer thickness. While both efficiency and fill factor (FF) exhibit a dependence on this parameter, their trends are opposing. We observe an increase in FF with increasing window layer thickness. This can be attributed to the reduction in recombination losses at the junction and improve the electrical properties.

Nevertheless, the same trend leads to a decrease in overall cell efficiency. Maybe as the window layer thickness increases, a greater portion of the incident light is absorbed within the ZnO layer before reaching the absorber layer (CZTS). This reduces the number of photons available for generating electron-hole pairs within the CZTS, ultimately leading to a decline in photocurrent and overall efficiency.

C. *Investigating the Impact of Buffer Layer Materials on CZTS Solar Cell Performance*

This study explores the influence of various n-type buffer layer materials on the performance and conversion efficiency of CZTS solar cells using a simulated device configuration depicted in Fig. 1. All other device parameters are held constant, allowing for a focused investigation on the effect of buffer layer material properties. The specific experimental parameters and material properties of the different n-type materials employed in the simulations are detailed in Table IV for reference. Cadmium sulfide (CdS) remains the most commonly used n-type material in CZTS solar cells, even in devices achieving the highest reported efficiencies [11]. Heterojunction band alignment has a pivotal role in overall efficiency. In case of CZTS/CdS solar cell both cliff and spike like configuration is reported. Both configuration has their own advantages and disadvantages which inhibits the efficiency of the cell. Thus it is essential to find the alternative n-material for the formation of favorable heterojunction band alignment. In the current study, different n-type material like ZnS, CdZnS, In_2S_3 and ZnSe is studies and reported.

Fig. 8 shows the device characteristics of CZTS based solar cell with different n-type materials. Black color square represents the cell efficiency and suggest that the efficiency of ZnS, In_2S_3 and WS_2 based cell are almost same as CdS and thus can be used n-type material in case of CZTS based solar cell. ZnS is not only a good alternative as it is non-toxic material but also it is cost efficient compare to CdS, In_2S_3 and WS_2. The reason for low efficiency in case of CdZnS and ZnSe based cell is lower short circuit current of the device. From Fig. 8, it is clear that short circuit current of CdZnS and ZnSe based cell is very less compare to other devices, limiting the overall efficiency.

D. *Enhancing CZTS Properties through Antimony (Sb) Doping*

Substitution of Sb for Sn in CZTS can tune the materials properties by modifying the electronics structure. Antimony has different electronic properties compared to tin, which can lead to changes in the band structure and the behavior of charge carriers within the material. This substitution can potentially enhance the absorption of sunlight and improve the efficiency of solar cells based on CZTS. Furthermore, limited performance of CZTS is due to its complex structure and presence of antisite defects such as Cu- Zn, Cu-Sn etc.

In 2017, Zhang et al. [26] elucidated the potential mechanism behind the enhanced efficiency of Sb-doped CZTS solar cells. Substitution of Sb for Sn in CZTS enhances the cell efficiency, J_{sc} and V_{oc} by introducing the intermediate band above Valence band maxima (VBM), which increases the photocurrent and improves the overall performance of the cell [26]."

Motivated by these theoretical predictions, we employed SCAPS-1D to investigate the influence of Sb substitution on CZTS solar cell performance. The specific device parameters used in this simulation study are detailed in Table V.

Anticipating significant variation in the antisite defect with increasing Sb concentration in CZTS, defect density of

TABLE IV
MATERIALS PARAMETERS OF DIFFERENT N-TYPE MATERIALS USED TO DESIGN DEVICE STRUCTURE

Parameters	CZTS	CdS	ZnS	CdZnS	In_2S_3	ZnSe	WS_2
Thickness	2	0.05	0.05	0.05	0.05	0.05	0.05
Bandgap (eV)	1.5	2.4	3.3	2.98	2.82	2.9	2.2
Electron Affinity χ	4.5	4.5	4.1	4.2	4.5	4.02	4.7
Dielectric permittivity ε	10	10	10	9.4	13.5	10	5.1
CB density of state	2.2E18	2.2E18	2.2E18	2.2E18	2.2E17	2.2E18	9.7E18
VB density of state	1.8E19	1.8E19	1.8E19	1.8E19	1.8E19	1.8E19	1.34E19
Electron thermal velocity	1.0E7	1.0E7	1.0E7	1.0E7	1.0E7	1.0E7	1.0E7
Hole thermal velocity	1.0E7	1.0E7	1.0E7	1.0E7	1.0E7	1.0E7	1.0E7
Electron mobility	1.0E2	1.0E2	1.0E2	2.7E2	1.0E2	2.5E1	1.0E2
Hole mobility	2.5E1	2.5E1	2.5E1	2.7E1	2.5E1	1.0E2	2.5E1
Donor density	1.0E1	1.0E18	1.0E18	1.0E17	1.0E13	1.0E17	1.0E18
Acceptor density	1.0E18	0	0	0	1.0E1	0	1.0E15

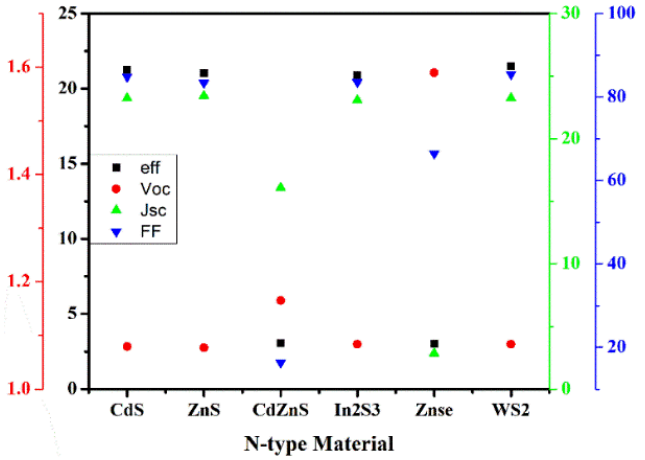

Fig. 8. Device characteristics of Mo/CZTS/CdS/ZnO solar cell using various n-type semiconductors.

CZTS is adjusted from 5E14 to 5E13 for Sb doped CZTS. Fig. 9 shows the J-V curve of Mo/Sb-CZTS/CdS/ZnO cell. Fig. 9 presents the current density-voltage (J-V) curve for the simulated Mo/Sb-doped CZTS/CdS/ZnO solar cell. The simulated device exhibits an open-circuit voltage (Voc) of 0.7026 V, a short-circuit current density (Jsc) of 40.08 mA/cm², and a corresponding efficiency of 21.90%. Hence, the boost in efficiency resulting from Sb doping in CZTS amounts to approximately 3% compare to undoped CZTS based solar cell, marking a significant advancement in the field of thin-film single-junction solar cells.

Fig. 10 illustrates the simulated External Quantum Efficiency (QE) of the solar cell across the ultraviolet-visible (UV-Vis) spectrum. Compared to the undoped CZTS cell (refer to Fig. 3 for reference), the Sb-doped cell exhibits an extended light absorption range. Notably, the QE remains

TABLE V
MATERIALS PARAMETERS USED IN CASE OF SB DOPED CZTS

Parameters	*Sb doped CZTS*	*CdS*	*ZnO*
Thickness (μm)	2	0.05	0.08
Bandgap (eV)	1.14	2.4	3.3
Electron Affinity χ	4.35	4.5	4.6
Dielectric permittivity ε	13.6	10	9.0
CB density of state	2.2E18	2.2E18	2.2E18
VB density of state	1.8E19	1.8E19	1.8E19
Electron thermal velocity	1.0E7	1.0E7	1.0E7
Hole thermal velocity	1.0E7	1.0E7	1.0E7
Electron mobility	1.0E2	1.0E2	1.0E2
Hole mobility	2.5E1	2.5E1	2.5E1
Donor density	1.0E1	1.0E18	1.0E18
Acceptor density	1.0E17	0	1.0E1

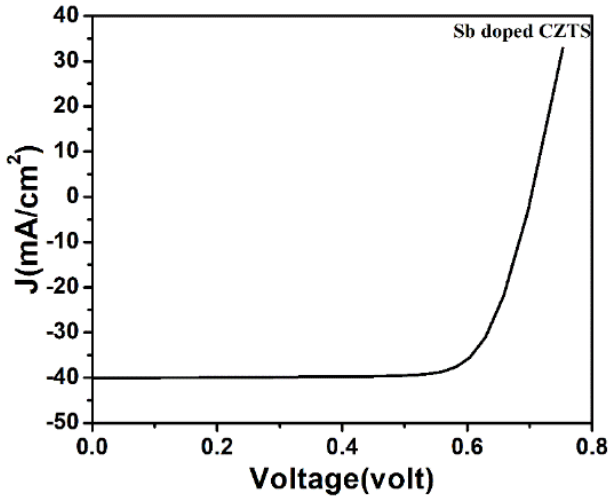

Fig. 9. J-V curve of Mo/Sb-CZTS/CdS/ZnO cell.

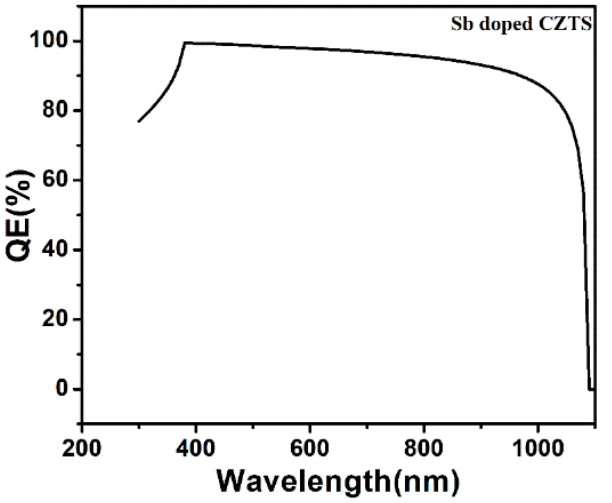

Fig. 10. Quantum Efficiency (QE) versus wavelength of Mo/Sb-CZTS/CdS/ZnO cell.

above 10% up to a wavelength of 1000 nm, as opposed to the 830 nm limit observed for the undoped device (Fig. 3). This signifies a significant improvement in light utilization by the Sb-doped CZTS solar cell. By effectively harvesting a broader range of light within the solar spectrum, Sb doping has the potential to contribute to the observed enhancement in overall device efficiency. Fig. 11 illustrates the simulated band

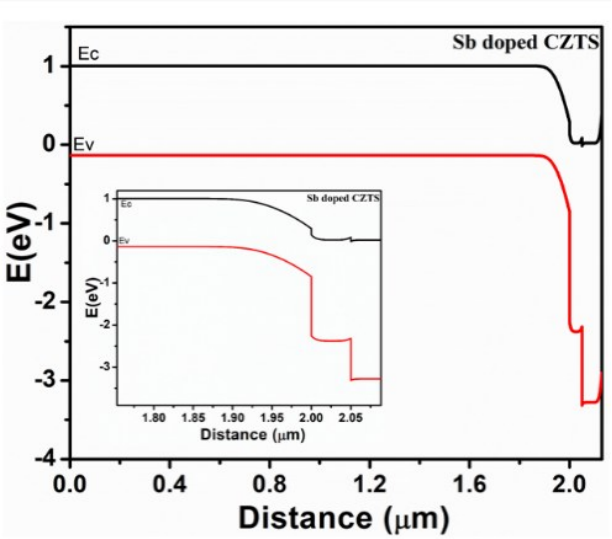

Fig. 11. Band alignment of Mo/Sb-CZTS/CdS/ZnO solar cell.

alignment for the Mo/Sb-CZTS/CdS/ZnO solar cell. The band alignment at the critical CZTS/CdS interface, which forms the heterojunction, appears largely unaffected by the Sb doping within the CZTS layer.

IV. CONCLUSION

This study employed numerical simulations to comprehensively investigate the device parameters of Mo/CZTS/CdS/ZnO thin-film solar cells. The simulations revealed that various parameters, including the thickness of the CZTS, CdS, and ZnO layers and impact of different buffer layer materials, significantly impact cell performance. The study additionally investigated the effects of Sb cation substitution within the CZTS structure. The results demonstrated a notable improvement in solar cell efficiency with Sb doping, suggesting this approach as a viable strategy for further efficiency enhancements. These findings hold significant potential for the development of next-generation high-efficiency solar cells. In the future, experimental studies of Sb doped CZTS solar cells are proposed for validation based on the SCAPS 1D simulation findings which suggest the improved efficiency of the cell. It includes synthesis of Sb doped CZTS material using non-vacuum techniques followed by the characterization to confirm the formation of Sb-doped CZTS material. Further, fabrication of Sb doped CZTS device is proposed to assess the Jsc, Voc, FF and efficiency of the cell under AM 1.5G condition. Formation of intermediate band above Valence band Maxima will be validated by the first-principles DFT calculations. Simulation results will be compared with experimental results to confirm the practical implementation of Sb-CZTS based solar cell.

REFERENCES

[1] Élodie de l'Épine and Ignacio Landivar, "2024 PV Trends: Global growth and challenges," PV Magazine International, Nov. 12, 2024. [Online]. Available: https://www.pv-magazine.com/2024/11/12/2024-pv-trends-global-growth-and-challenges.

[2] S. H. Zyoud et al., "Effect of Absorber (Acceptor) and Buffer (Donor) Layers Thickness on Mo/CdTe/CdS/ITO Thin Film Solar Cell Performance: SCAPS-1D Simulation Aspect," I.RE.MO.S., vol. 14 (1), pp. 10-17, Aprl 2021. doi:https://doi.org/10.15866/iremos.v14i1.19953

[3] S. H. Zyoud et al., "Numerical Modelling Analysis for Carrier Concentration Level Optimization of CdTe Heterojunction Thin Film–Based Solar Cell with Different Non–Toxic Metal Chalcogenide Buffer Layers Replacements: Using SCAPS–1D Software," Crystals, vol. 11 (12), pp. 1454, Dec 2021. https://doi.org/10.3390/cryst11121454https://doi.org/10.3390/cryst11121454

[4] S. H. Zyoud et al., "Simulation and Numerical Investigation of the Effect of Temperature and Defect on ZnTe/ZnSe/ZnO Thin-Film Photovoltaic Solar Cell Performance Efficiency," IREA, vol. 11, pp. 1-10 Jan 2023. https://doi.org/10.15866/irea.v11i1.20839

[5] M. S. Aljuboori et al., ''Enhancing Photoconversion Efficiency by Optimization of Electron/Hole Transport Interlayers in Antimony Sulfide Solar Cell using SCAPS-1D Simulation,'' JSESD, vol. 13 (1), pp. 97-113 Jun 2024. https://doi.org/10.51646/jsesd.v13i1.175

[6] Mubarak H. O. et al., "Simulation Analysis for the Efficiency Enhancement of Sb_2S_3 Solar Cell Using SCAPS-1D," CMMS, vol. 23 (4), pp. 19-29 2023. https://doi.org/10.7494/cmms.2023.4.0817

[7] S. H. Zyoud et al., "Numerical Simulation for Optimization of ZnTe-Based Thin-Film Heterojunction Solar Cells with Different Metal Chalcogenide Buffer Layers Replacements: SCAPS-1D Simulation Program," I.RE.MO.S., Vol. 14 (2), pp. 79-88 Aprl 2021. https://doi.org/10.15866/iremos.v14i2.19954

[8] S. H. Zyoud et al., "Investigating the impact of temperature and interlayer defects on the efficiency of Mo/ZnTe/ZnSe/SnO_2 heterojunction thin-film solar cells: A SCAPS-1D simulation study," I.RE.MO.S., vol. 16(3), pp. 120-128 June 2023. https://doi.org/10.15866/iremos.v16i3.22739

[9] S. H. Zyoud et al., "Numerical Modeling of High Conversion Efficiency FTO/ZnO/CdS/CZTS/MO Thin Film-Based Solar Cells: Using SCAPS-1D Software," Crystals, vol. 11, pp. 1468 (1-21) Nov 2021. https://doi.org/10.3390/cryst11121468

[10] Xin Cui et al., "Cd-Free Cu_2ZnSnS_4 solar cell with an efficiency greater than 10% enabled by Al_2O_3 passivation layers," Energy Environ. Sci., vol. 12, pp. 2751-2764 July 2019. https://doi.org/10.1039/C9EE01726G

[11] Wei Wang et al., "Device Characteristics of CZTSSe Thin-Film Solar Cells with 12.6% Efficiency," Adv Energy Mater., vol. 4(7), pp. 1301465 (1-5) Nov 2013. https://doi.org/10.1002/aenm.201301465

[12] H.-Q. Xiao et al., "Boosting the efficiency of solution-based CZTSSe solar cells by supercritical carbon dioxide treatment," Green Chem., vol. 22, pp. 3597-3607 May 2020. https://doi.org/10.1039/D0GC01355B

[13] S. Zhuk et al., "Critical review on sputter-deposited Cu_2ZnSnS_4 (CZTS) based thin-film photovoltaic technology focusing on device architecture and absorber quality on the solar cells performance," Sol. Energy Mater. Sol. Cells, vol. 171, pp. 239-252 Nov 2017. https://doi.org/10.1016/j.solmat.2017.05.064.

[14] Kannan P. K. et al., "Detailed investigations on influence of precursor stacking and sulfurization for Cu_2ZnSnS_4 film formation," Thin Solid Films, vol. 649, pp. 81-88 Mar 2018. https://doi.org/10.1016/j.tsf.2018.01.038.

[15] Kannan P. K. et al., "Effect of anionic substitution of S by Se in CZTSSe films prepared from electron beam evaporation," Mater. Today Proc., vol. 21 (4), pp. 1787-1792 2020. https://doi.org/10.1016/j.matpr.2020.01.232.

[16] S. Chaudhari et al., "Investigation of optimum annealing parameters for formation of dip-coated Cu_2ZnSnS_4 thin film," Thin Solid Films, vol. 612, pp. 456-462 Aug 2016. https://doi.org/10.1016/j.tsf.2016.06.046.

[17] S. Chaudhari et al., "Influence of stabilizing agent on dip coating of Cu_2ZnSnS_4 thin film," Thin Solid Films, vol. 636, pp. 144-149 Aug 2017. https://doi.org/10.1016/j.tsf.2017.05.045.

[18] S. Chaudhari et al., "Formulation of selenium-rich $Cu_2ZnSn(S_xSe_{1-x})_4$ film through non-vacuum dip coating technique," J. Mater. Sci.: Mater. Electron., vol. 32, pp. 19102-19109 July 2021. https://doi.org/10.1007/s10854-021-06427-y.

[19] K. Madhuri et al., "Investigations on treatments on CIGS formation using spin-coated CIG precursor," J. Mater. Sci.: Mater. Electron., vol. 32, pp. 1521-1527 Jan 2021. https://doi.org/10.1007/s10854-020-04921-3.

[20] S. Chaudhari et al., "Pulsed electrodeposition of Cu_2ZnSnS_4 absorber layer precursor for photovoltaic application," Thin Solid Films, vol. 600, pp. 169-174 Feb 2016. https://doi.org/10.1016/j.tsf.2016.01.021.

[21] S. H. Zyoud et al., "Influence of the redox couple concentration and activity of a NaOH/Na_2S/S electrolyte on the performance of CdS thin-film photoelectrochemical cells," Chem. Eng. J., vol. 10, pp. 100864 (1-9) Dec 2024. https://doi.org/10.1016/j.cscee.2024.100864.

[22] A. Zyoud et al., "Enhanced PEC characteristics of pre-annealed CuS film electrodes by metalloporphyrin/polymer matrices," Solar Energy Mater. Solar Cells, vol. 144, pp. 429-437 Jan 2016. https://doi.org/10.1016/j.solmat.2015.09.034.

[23] A. Zyoud et al., "High PEC conversion efficiencies from CuSe film electrodes modified with metalloporphyrin/polyethylene matrices," Electrochimica Acta, vol. 174, pp. 472-479 Aug 2015. https://doi.org/10.1016/j.electacta.2015.05.125.

[24] H. Sabri et al., "Enhancement of CdSe film electrode PEC characteristics by metalloporphyrin/polysiloxane matrices," Electrochimica Acta, vol. 136, pp. 138-145, Aug 2014. https://doi.org/10.1016/j.electacta.2014.05.071.

[25] A. Zyoud et al., "Enhanced PEC characteristics for CdSe polycrystalline film electrodes prepared by combined electrochemical/chemical bath depositions," J. Electroanal. Chem., vol. 774, pp. 7-13, Aug 2016. https://doi.org/10.1016/j.jelechem.2016.04.048.

[26] Xiaoli Zhang, Miaomiao Han, Zhi Zeng and Yuhua Duan, "The role of Sb in solar cell material Cu_2ZnSnS_4," J. Mater. Chem A, vol. 5, pp. 6606-6612 Mar 2017. https://doi.org/10.1039/C7TA01090G

[27] Kannan P.K. and Mariappan Anandkumar, "A theoretical investigation to boost the efficiency of CZTS solar cells using SCAPS-1D," Optik, vol. 288, pp. 171214 Oct 2023. https://doi.org/10.1016/j.ijleo.2023.171214.

[28] S. Siebentritt, "Why are kesterite solar cells not 20% efficient?," Thin Solid Films, vol 535, pp. 1-4 May 2013. https://doi.org/10.1016/j.tsf.2012.12.089

[29] Touria Ouslimane, Lhoussayne Et-taya, Lahoucine Elmaimouni, Abdellah Benami, "Impact of absorber layer thickness, defect density, and operating temperature on the performance of $MAPbI_3$ solar cells based on ZnO electron transporting material," Heliyon, vol. 7, pp. e06379 (1-6) Mar 2021. https://doi.org/10.1016/j.heliyon.2021.e06379

[30] Maykel Courel, J A Andrade-Arvizu and O Vigil-Galán, "The role of buffer/kesterite interface recombination and minority carrier lifetime on kesterite thin film solar cells, " Mater. Res. Express vol. 3 pp. 095501 (1-15) Sep 2016. https://doi.org/ 10.1088/2053-1591/3/9/095501

Sushmita Chaudhari is an Assistant Professor in Computer Science and Engineering department Brainware University Barasat, Kolkata India. She received her Ph.D. degree from Indian Institute of Technology Hyderabad. Her research interests include fabrication of semiconductor materials and its characterization. Additionally, Simulation and prediction of photovoltaic cell performance based on its layer by layer properties using SCAPS 1D.

Kannan P. K. is a renowned professor and researcher working in the field of Materials Science and Engineering. He received his PhD from the Indian Institute of Technology Hyderabad. At present, he works as an Assistant Professor (Senior Grade) in the Department of Physics at PSG Institute of Technology and Applied Research, Coimbatore, India. Dr. Kannan's research interest includes photovoltaic materials, high entropy oxides, perovskite etc.